A simple RNA-DNA scaffold templates the assembly of monofunctional virus-like particles

Rees F. Garmann[1,†], Richard Sportsman[1], Christian Beren[1], Vinothan N. Manoharan[4,5], Charles M. Knobler[1], William M. Gelbart[1,2,3,*]

[1]*Department of Chemistry and Biochemistry,* [2]*California NanoSystems Institute, and* [3]*Molecular Biology Institute, University of California, Los Angeles, Los Angeles, CA 90095, USA.*

[4]*School of Engineering and Applied Sciences, and* [5]*Department of Physics, Harvard University, Cambridge, MA 02138, USA.*

ABSTRACT: Using the components of a particularly well-studied plant virus, cowpea chlorotic mottle virus (CCMV), we demonstrate the synthesis of virus-like particles (VLPs) with one end of the packaged RNA extending out of the capsid and into the surrounding solution. This construct breaks the otherwise perfect symmetry of the capsid and provides a straightforward route for monofunctionalizing VLPs using the principles of DNA nanotechnology. It also allows physical manipulation of the packaged RNA, a previously inaccessible part of the viral architecture. Our synthesis does not involve covalent chemistry of any kind; rather, we trigger capsid assembly on a scaffold of viral RNA that is hybridized at one end to a complementary DNA strand. Interaction of CCMV capsid protein with this RNA-DNA template leads to selective packaging of the RNA portion into a well-formed capsid, but leaves the hybridized portion poking out of the capsid through a small hole. We show that the nucleic acid protruding from the capsid is capable of binding free DNA strands and DNA-functionalized colloidal particles. Separately, we show that the RNA-DNA scaffold can be used to nucleate virus formation on a DNA-functionalized surface. We believe this self-assembly strategy can be adapted to viruses other than CCMV.

Small RNA viruses consist entirely of genomic RNA packaged inside a one-molecule-thick protective protein capsid (Fig.1). In addition to making up a large fraction of the world's viral pathogens, small RNA viruses are helping to define new fields of applied science through their use as functional nanoparticles[1]. For example, they have been exploited as contrast agents for biomedical imaging[2–5], as vectors for the delivery of small molecules and genes to cells[6–11], and as nanoscale building blocks for the formation of superstructures with unique material, optical and dynamic properties[12–17].

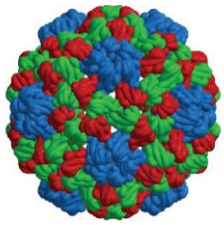

Figure 1. The capsid of cowpea chlorotic mottle virus (CCMV), like many small RNA viruses, has icosahedral symmetry and consists of 180 copies of its capsid protein. Diameter is 28 nm. Taken from VIPERdb[18].

Much of the utility of small RNA viruses derives from their symmetric capsids[19] which can be engineered to display a high density of functional moieties. Indeed, an arsenal of functionalization strategies[20–31] has been developed that combine molecular biology (cloning) and/or selective covalent chemistries to isotropically label the various polyvalent surfaces (exterior, interior, and interfacial[1]) of the capsid. However, in situations where a high degree of labeling is not desired, *mono*functional particles that display only a single copy (or a specific limited arrangement) of a particular functional group are needed. Not surprisingly, monofunctional virus

doi: 10.1021/jacs.5b03770

particles are difficult to produce[32–34] in a controlled way due to the inherent symmetry of the capsid and its abundance of equivalent binding sites.

Lying just beneath the capsid, the viral RNA contains a wealth of inequivalent binding sites that could in principle be selectively targeted using the methods of DNA nanotechnology[35–40]. Unfortunately, the capsid is impermeable to these techniques – the main evolutionary purpose of the capsid is to protect the RNA from unfavorable interactions with macromolecules from the outside world. Our work bypasses this inaccessibility through the synthesis of virus-like particles (VLPs) with a portion of one end of the RNA extending outside of the capsid (Fig. 2). With the symmetry of the particle broken by the exposed RNA, we generate robust monofunctionalization through the conjugation of desired moieties using only Watson-Crick basepairing.

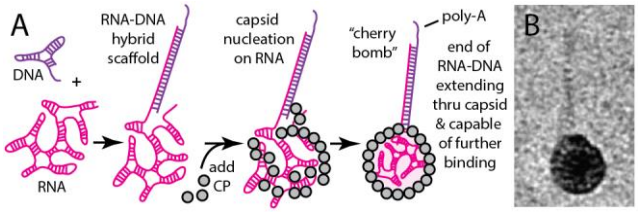

Figure 2. (A) Schematic illustration of assembly of the "cherry bomb". (B) Positive-stain transmission electron micrograph (TEM) of a cherry bomb capsid (dark sphere measuring 26 nm) and its RNA-DNA appendage (lighter strand extending upward).

Our synthesis (Fig. 2A) requires neither genetic modification nor covalent chemistry, but instead relies on the ability of a particularly well-studied small RNA virus, CCMV, to be disassembled and reconstituted by self-assembly *in vitro*[41]. Additionally, we exploit the qualitative structural differences between single-stranded (ss) and double-stranded (ds) nucleic acid to reshape the viral RNA that templates the assembly.

Owing to extensive intramolecular base pairing, ss-RNA of the length naturally packaged by CCMV (about 3 kb) is a highly branched, flexible, compact object that has physical dimensions comparable to the capsid interior[42] (22-nm-internal diameter). In contrast, the same length (3 kbp) of ds-DNA occupies a much larger volume owing to its increased stiffness (~50 nm persistence length) and lack of branching. As a result, ds-DNA longer than about 75 bp cannot be accommodated within the interior volume of the CCMV capsid and does not function as a template for normal capsid assembly[43,44].

By hybridizing the first 185 bases at the 5'-end of a 3.2 kb ss-RNA with a complementary ss-DNA strand, we dramatically stiffen the 5'-end of the RNA. [We use the 5'-end of the 3234-base RNA molecule ("B1") of the tripartite genome of brome mosaic virus (BMV), although either end of any similar-length sequence will likely do.] Here, the DNA strand (see SI) acts as a molecular splint. The resulting RNA-DNA hybrid can be expected to behave as a compact, flexible, branched 3-kb ss-RNA connected to a rigid, linear, 185-base ds-RNA-DNA appendage (see 2nd-from-left cartoon in Fig. 2A). The physical length of the ds portion is about 50 nm. It is very stable (85ºC melting temperature) owing to its perfect sequence complementarity.

The *in vitro* packaging of this RNA-DNA hybrid by CCMV capsid protein (CP), using the same protocol developed earlier for pure RNA[45–47], results in the selective encapsidation of the ss-RNA portion and leaves the ds-RNA-DNA appendage poking out of the capsid and into solution. We refer to this final construct as a "cherry bomb" because of its structural resemblance (Fig. 2B, additional images shown in SI, Fig. S1) to the well-known explosive firework[48].

While the structure of the hole that passes the ds-RNA-DNA through the capsid is not known, previous *in vitro* packaging studies have shown ss and ds nucleic acid traversing the capsids of CCMV and the closely related BMV. We previously observed[49] that ss-RNA molecules significantly longer than wild-type are packaged by multiple CCMV capsids ("multiplets") that each share a portion of the overlong RNA (Fig. 3). And a separate study[44] found that long ds-DNA is packaged by a contiguous string of many BMV capsids if ss-RNA fragments are also present. In both cases nucleic acid is shared by connected capsids, passing through one or more holes in each capsid that are too small to be seen by negative-stain TEM. It is likely that the ds-RNA-DNA appendage of the cherry bomb exits the capsid through a similar hole.

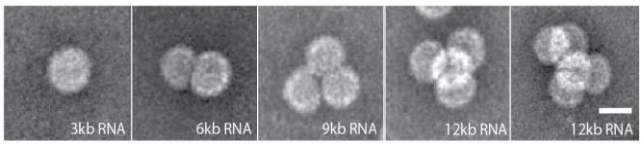

Figure 3. Single ss-RNA molecules progressively longer than wild-type (3kb) are shared by two or more CCMV capsids – multiplets[49]. Scale bar shows 25 nm. Copyright © American Society for Microbiology, [Journal of Virology, 86, 2012, 3322, doi:10.1128/JVI.06566-11].

To test whether the exposed RNA-DNA appendage can be used to bind nucleic acids in solution, we designed the DNA splint with a 3' poly-A_{15} overhang in addition to the 185 bases that complement the 5'-end of the RNA (see right-most cartoon in Fig. 2A). Once formed, cherry bombs were combined with fluorescent (green) ss-poly-T_{15} DNA strands and analyzed by native agarose gel electrophoresis (Fig. 4). The cherry bombs and the fluorescent poly-T_{15} co-migrated (Fig. 4, lane 3), confirming that the poly-A_{15} sticky end of the RNA-DNA appendage binds its complementary strand in solution. Control experiments in which *already*-assembled VLPs containing only 3.2 kb RNA (B1) were added to the splint DNA and fluorescent poly-T_{15} showed no nonspecific binding (Fig. 4, lane 4).

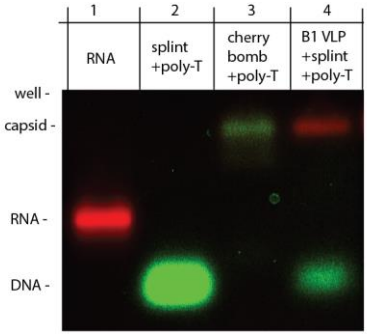

Figure 4. Native agarose gel electrophoresis shows cherry bombs selectively bind fluorescently labeled poly-T_{15} DNA strands (green). Fluorescently labeled RNA shown in red.

The ability of the cherry bomb to bind a functionalized surface was demonstrated by direct imaging of a mixture of these capsids with 30-nm gold nanoparticles (AuNPs) that had been previously decorated with a high density of ss-poly-T_{25} DNA strands[50] (Fig. S2). Negative-stain TEM (Fig. 5) shows a high concentration of capsids at the AuNP surface, and an exceptionally well-stained image reveals the RNA-DNA appendage linking the capsids to the gold surface (Fig. 5, arrows). Control experiments between B1 VLPs and functionalized AuNPs showed no non-specific binding (Fig. S3).

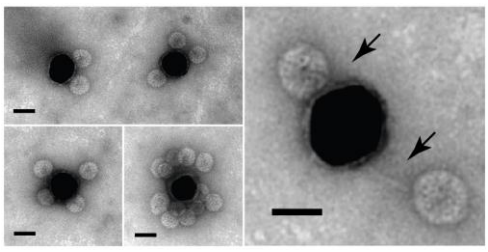

Figure 5. Cherry bomb capsids bind the surface of DNA-functionalized 30-nm AuNPs. A zoomed-in transmission electron micrograph resolves the RNA-DNA duplex (arrows) linking the capsids (light spheres) and the AuNPs (dark sphere). Scale bars show 25 nm.

Separately, we tested whether capsids could be assembled around RNAs that were already tethered to a functionalized surface (Fig. 6A). Here, the hybrid RNA-DNA scaffold was prepared and equilibrated with 30-nm poly-T_{25}-coated AuNPs at a molar ratio of 10:1 (RNA:AuNP). After hybridization of the RNA to the AuNPs, CP was added at a mass ratio of 10:1 (CP:RNA), equilibrated for 5 min on ice, and imaged by negative-stain TEM (Fig. 6B). The presence of well-defined capsids at the Au particle surface demonstrated assembly of cherry bomb capsids around the immobilized RNA-DNA. Some aggregation of CP in the presence of AuNPs was also observed (Fig. S4).

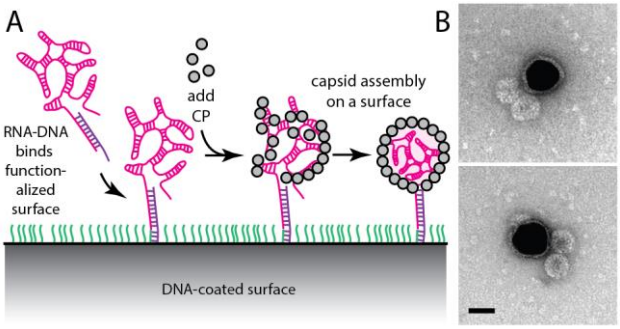

Figure 6. (A) Schematic showing the assembly of VLPs on a DNA-functionalized (green strands) surface. (B) Electron micrographs of cherry bomb capsids (light spheres) grown on 30-nm AuNPs (dark spheres) as shown in (A). Scale bar shows 25 nm.

While several elegant methods have recently been described for the monofunctionalization of tobacco mosaic virus particles[51–53], they most likely cannot be applied to other viruses – they require either controlled disassembly of one end of the rod-like capsid or self-assembly of capsids on a substrate-bound RNA that contains a specific packaging sequence. The homogeneous assembly pathway described here provides a general strategy for monofunctionalizing icosahedral particles. Here we note that the ability to form cherry bomb structures is probably not limited to the plant virus CCMV; multiplet capsids have been observed in the packaging of overlong RNAs by the CP of the bacterial virus fr[54] and of the mammalian virus SV40[55], indicating that they too have the potential to form cherry bombs.

In addition to offering a single, highly-specific, binding modality for building functional viral-based materials, our method for (i) physically binding and manipulating one end of the packaged genome and (ii) nucleating capsid assembly at a surface will enable new single-particle measurements that might reveal how RNA gets into and out of viral capsids during infection. Examples of such measurements include time-resolved studies of capsid assembly, and force-pulling experiments[56,57] that measure the work required to pull viral RNA out of its capsid.

ASSOCIATED CONTENT

Supporting Information. Procedures and additional data are available free of charge via the Internet at http://pubs.acs.org.

AUTHOR INFORMATION

Corresponding Author

*gelbart@chem.ucla.edu.

Present Addresses

†School of Engineering and Applied Sciences, Harvard University, Cambridge, MA 02138, USA.

ACKNOWLEDGMENT

WMG and CMK acknowledge support from the NSF through grant CHE 1051507. VNM acknowledges support from the NSF through grant no. DMR-1435964. TEM images were obtained in the California NanoSystems Institute Electron Imaging Center for Nano-Machines, supported by NIH (1S10RR23057). Additional support provided by an NIH training grant for USPHS National Research Service Award 5T32GM008496.

REFERENCES

(1) Douglas, T.; Young, M. *Science* **2006**, *312* (5775), 873.
(2) Liepold, L.; Anderson, S.; Willits, D.; Oltrogge, L.; Frank, J. A.; Douglas, T.; Young, M. *Magn. Reson. Med.* **2007**, *58* (5), 871.
(3) Malyutin, A. G.; Easterday, R.; Lozovyy, Y.; Spilotros, A.; Cheng, H.; Sanchez-Felix, O. R.; Stein, B. D.; Morgan, D. G.; Svergun, D. I.; Dragnea, B.; Bronstein, L. M. *Chem. Mater.* **2014**.
(4) Prasuhn, D. E.; Yeh, R. M.; Obenaus, A.; Manchester, M.; Finn, M. G. *Chem. Commun. Camb. Engl.* **2007**, No. 12, 1269.
(5) Datta, A.; Hooker, J. M.; Botta, M.; Francis, M. B.; Aime, S.; Raymond, K. N. *J. Am. Chem. Soc.* **2008**, *130* (8), 2546.
(6) Aljabali, A. A.; Shukla, S.; Lomonossoff, G. P.; Steinmetz, N. F.; Evans, D. J. *Mol. Pharm.* **2012**, *10* (1), 3.
(7) Azizgolshani, O.; Garmann, R. F.; Cadena-Nava, R.; Knobler, C. M.; Gelbart, W. M. *Virology* **2013**, *441* (1), 12.
(8) Destito, G.; Yeh, R.; Rae, C. S.; Finn, M. G.; Manchester, M. *Chem. Biol.* **2007**, *14* (10), 1152.
(9) Brown, W. L.; Mastico, R. A.; Wu, M.; Heal, K. G.; Adams, C. J.; Murray, J. B.; Simpson, J. C.; Lord, J. M.; Taylor-Robinson, A. W.; Stockley, P. G. *Intervirology* **2003**, *45* (4-6), 371.
(10) Wu, M.; Brown, W. L.; Stockley, P. G. *Bioconjug. Chem.* **1995**, *6* (5), 587.
(11) Wu, M.; Sherwin, T.; Brown, W. L.; Stockley, P. G. *Nanomedicine Nanotechnol. Biol. Med.* **2005**, *1* (1), 67.
(12) Chen, C.; Daniel, M.-C.; Quinkert, Z. T.; De, M.; Stein, B.; Bowman, V. D.; Chipman, P. R.; Rotello, V. M.; Kao, C. C.; Dragnea, B. *Nano Lett.* **2006**, *6* (4), 611.
(13) Maye, M. M. *Nat. Nanotechnol.* **2013**, *8* (1), 5.
(14) Kostiainen, M. A.; Kasyutich, O.; Cornelissen, J. J.; Nolte, R. J. *Nat. Chem.* **2010**, *2* (5), 394.
(15) Dixit, S. K.; Goicochea, N. L.; Daniel, M.-C.; Murali, A.; Bronstein, L.; De, M.; Stein, B.; Rotello, V. M.; Kao, C. C.; Dragnea, B. *Nano Lett.* **2006**, *6* (9), 1993.
(16) Wang, Q.; Lin, T.; Johnson, J. E.; Finn, M. G. *Chem. Biol.* **2002**, *9* (7), 813.
(17) Cadena-Nava, R. D.; Hu, Y.; Garmann, R. F.; Ng, B.; Zelikin, A. N.; Knobler, C. M.; Gelbart, W. M. *J. Phys. Chem. B* **2011**, *115* (10), 2386.
(18) http://viperdb.scripps.edu/.
(19) Carrillo-Tripp, M.; Shepherd, C. M.; Borelli, I. A.; Venkataraman, S.; Lander, G.; Natarajan, P.; Johnson, J. E.; Brooks, C. L.; Reddy, V. S. *Nucleic Acids Res.* **2009**, *37* (suppl 1), D436.
(20) Gillitzer, E.; Willits, D.; Young, M.; Douglas, T. *Chem Commun* **2002**, No. 20, 2390.
(21) Blum, A. S.; Soto, C. M.; Wilson, C. D.; Cole, J. D.; Kim, M.; Gnade, B.; Chatterji, A.; Ochoa, W. F.; Lin, T.; Johnson, J. E.; others. *Nano Lett.* **2004**, *4* (5), 867.
(22) Strable, E.; Finn, M. G. In *Viruses and Nanotechnology*; Springer, 2009; pp 1–21.
(23) Steinmetz, N. F.; Lomonossoff, G. P.; Evans, D. J. *Langmuir* **2006**, *22* (8), 3488.
(24) Smith, J. C.; Lee, K.-B.; Wang, Q.; Finn, M. G.; Johnson, J. E.; Mrksich, M.; Mirkin, C. A. *Nano Lett.* **2003**, *3* (7), 883.
(25) Raja, K. S.; Wang, Q.; Gonzalez, M. J.; Manchester, M.; Johnson, J. E.; Finn, M. G. *Biomacromolecules* **2003**, *4* (3), 472.
(26) Gupta, S. S.; Raja, K. S.; Kaltgrad, E.; Strable, E.; Finn, M. G. *Chem. Commun.* **2005**, No. 34, 4315.
(27) Pokorski, J. K.; Breitenkamp, K.; Finn, M. G. *J. Am. Chem. Soc.* **2011**, *133* (24), 9242.
(28) Pokorski, J. K.; Steinmetz, N. F. *Mol. Pharm.* **2011**, *8* (1), 29.
(29) Patel, K. G.; Swartz, J. R. *Bioconjug. Chem.* **2011**, *22* (3), 376.
(30) Steinmetz, N. F.; Lin, T.; Lomonossoff, G. P.; Johnson, J. E. In *Viruses and Nanotechnology*; Springer, 2009; pp 23–58.
(31) Young, M.; Debbie, W.; Uchida, M.; Douglas, T. *Annu Rev Phytopathol* **2008**, *46*, 361.
(32) Klem, M. T.; Willits, D.; Young, M.; Douglas, T. *J. Am. Chem. Soc.* **2003**, *125* (36), 10806.
(33) Suci, P. A.; Kang, S.; Young, M.; Douglas, T. *J. Am. Chem. Soc.* **2009**, *131* (26), 9164.
(34) Li, F.; Chen, Y.; Chen, H.; He, W.; Zhang, Z.-P.; Zhang, X.-E.; Wang, Q. *J. Am. Chem. Soc.* **2011**, *133* (50), 20040.
(35) Mirkin, C. A.; Letsinger, R. L.; Mucic, R. C.; Storhoff, J. J. *Nature* **1996**, *382* (6592), 607.
(36) Rothemund, P. W. K. *Nature* **2006**, *440* (7082), 297.
(37) Strable, E.; Johnson, J. E.; Finn, M. G. *Nano Lett.* **2004**, *4* (8), 1385.
(38) Stephanopoulos, N.; Liu, M.; Tong, G. J.; Li, Z.; Liu, Y.; Yan, H.; Francis, M. B. *Nano Lett.* **2010**, *10* (7), 2714.
(39) Wang, D.; Capehart, S. L.; Pal, S.; Liu, M.; Zhang, L.; Schuck, P. J.; Liu, Y.; Yan, H.; Francis, M. B.; De Yoreo, J. J. *ACS Nano* **2014**, *8* (8), 7896.
(40) Rogers, W. B.; Manoharan, V. N. *Science* **2015**, *347* (6222), 639.
(41) Bancroft, J. B.; Hiebert, E. *Virology* **1967**, *32* (2), 354.

(42) Gopal, A.; Zhou, Z. H.; Knobler, C. M.; Gelbart, W. M. *Rna* **2012**, *18* (2), 284.
(43) Mukherjee, S.; Pfeifer, C. M.; Johnson, J. M.; Liu, J.; Zlotnick, A. *J. Am. Chem. Soc.* **2006**, *128* (8), 2538.
(44) Pfeiffer, P.; Herzog, M.; Hirth, L. *Philos. Trans. R. Soc. Lond. B Biol. Sci.* **1976**, *276* (943), 99.
(45) Garmann, R. F.; Comas-Garcia, M.; Gopal, A.; Knobler, C. M.; Gelbart, W. M. *J. Mol. Biol.* **2014**, *426* (5), 1050.
(46) Garmann, R. F.; Comas-Garcia, M.; Koay, M. S.; Cornelissen, J. J.; Knobler, C. M.; Gelbart, W. M. *J. Virol.* **2014**, *88* (18), 10472.
(47) Comas-Garcia, M.; Garmann, R. F.; Singaram, S. W.; Ben-Shaul, A.; Knobler, C. M.; Gelbart, W. M. *J. Phys. Chem. B* **2014**, *118* (27), 7510.
(48) http://en.wikipedia.org/wiki/Cherry_bomb.
(49) Cadena-Nava, R. D.; Comas-Garcia, M.; Garmann, R. F.; Rao, A. L. N.; Knobler, C. M.; Gelbart, W. M. *J. Virol.* **2012**, *86* (6), 3318.
(50) Hurst, S. J.; Lytton-Jean, A. K.; Mirkin, C. A. *Anal. Chem.* **2006**, *78* (24), 8313.
(51) Yi, H.; Rubloff, G. W.; Culver, J. N. *Langmuir* **2007**, *23* (5), 2663.
(52) Eber, F. J.; Eiben, S.; Jeske, H.; Wege, C. *Angew. Chem. Int. Ed.* **2013**, *52* (28), 7203.
(53) Jung, S.; Yi, H. *Langmuir* **2014**, *30* (26), 7762.
(54) Hohn, T. *J. Mol. Biol.* **1969**, *43* (1), 191.
(55) Kler, S.; Wang, J. C.-Y.; Dhason, M.; Oppenheim, A.; Zlotnick, A. *ACS Chem. Biol.* **2013**, *8* (12), 2753.
(56) Smith, D. E.; Tans, S. J.; Smith, S. B.; Grimes, S.; Anderson, D. L.; Bustamante, C. *Nature* **2001**, *413* (6857), 748.
(57) Liu, N.; Peng, B.; Lin, Y.; Su, Z.; Niu, Z.; Wang, Q.; Zhang, W.; Li, H.; Shen, J. *J. Am. Chem. Soc.* **2010**, *132* (32), 11036.

Supporting information: A simple RNA-DNA scaffold templates the assembly of monofunctional virus-like particles

Rees F. Garmann[1,†], Richard Sportsman[1], Christian Beren[1], Vinothan N. Manoharan[4,5], Charles M. Knobler[1], William M. Gelbart[1,2,3,*]

[1]Department of Chemistry and Biochemistry, [2]California NanoSystems Institute, and [3]Molecular Biology Institute, University of California, Los Angeles, Los Angeles, CA 90095, USA.

[4]School of Engineering and Applied Sciences, and [5]Department of Physics, Harvard University, Cambridge, MA 02138, USA.

Synthesis of capsid protein

Capsid protein (CP) was purified from wild-type cowpea chlorotic mottle virus (CCMV) grown in California cowpea plants (*Vigna ungiculata* cv Black Eye) as described by Annamalai and Rao[1]. Briefly, virions were disrupted by 24-h dialysis against disassembly buffer (1M $CaCl_2$, 50 mM Tris pH 7.5, 1 mM EDTA, 1 mM DTT, and 0.5 mM PMSF) at 4°C. The RNA was pelleted by ultracentrifugation at 4 x 10^5 g for 90 min and the CP was extracted from the supernatant in separate fractions. Each fraction was immediately dialyzed against protein buffer (1M NaCl, 20 mM Tris pH = 7.2, 1 mM EDTA, 1 mM DTT, and 1 mM PMSF). The protein concentration and its purity, with respect to RNA contamination, were measured by UV-Vis spectrophotometry – only protein samples with 280/260 ratios greater than 1.5 (less than 5% RNA contamination) were used for assembly. SDS-PAGE gel electrophoresis and MALDI-TOF showed no evidence of cleaved protein.

Synthesis of RNA

Fluorecently labeled brome mosaic virus genomic RNA1 (B1) was synthesized by *in vitro* transcription of a linearized DNA template by T7 RNA polymerase and fluorecent rUTP-AF488 (Chroma-Tide® Alexa Fluor® 488-5-UTP; Molecular Probes, U.S.A.). A rATP:rGTP:rCTP:rUTP:rUTP-AF488 molar ratio of 600:600:600:5.32:1 was used and resulted in a density of labeling of 0.5 rUTP-AF488s per RNA. After transcription, the template DNA was digested by DNase I (New England Biolabs), and the resulting fragments removed by washing five times with a 20-fold excess of TE buffer (10mM Tris pH 7.5, 1 mM EDTA) using a 100 kDa MWCO centrifugal filter device (EMD Milipore) operated at 5,000 g.

Design and Synthesis of DNA

The DNA splint strand was purchased from Integrated DNA Technologies. The sequence is shown below:

5'-AATCTGCGCAGATAACTGTTGCGCGACCTGA
TTGTCTACGATGTCTTGGGCACTCTGGCTGGCA
GCACCCTTCTCAGCAATCAACTTCAGCAAATCG
ATAGAACTTGACATTTTGTTGGTGAAAAACAAAG
AACAAGTAGCAGAACCGTGGTCGACAAGGGAT
TGAACCTCGTTCCGTGGTCTACAAAAAAAAAAA
AAAA-3'

This sequence consists of the reverse complement of the first 185 bases of the 5' terminus of B1 RNA followed by poly-A_{15}.

We did not test whether DNA splints with complementary sequences shorter than 185-bases are capable of templating the assembly of cherry bombs, though we suspect this is the case. Assuming that the rise of hybridized ds-RNA-DNA is intermediate between those of ds-DNA (0.34 nm per bp) and ds-RNA (0.25nm per bp), the physical length of a 185 bp hybrid strand measures about 55 nm, 2-3 times the inner diameter (22 nm) of the CCMV capsid. Therefore, we expect that much shorter DNA splints (as short as, say, 80 bases) should lead to hybrid ds-RNA-DNA portions that are too long to be packaged. However, these cherry bombs would have "fuses" that extend a shorter distance from the capsid. Alternatively, multiple short DNA splints designed to bind adjacent RNA sequences might be used to generate a more flexible fuse, due to the nicks between each pair of neighboring splints.

doi: 10.1021/jacs.5b03770

Fluorescent Poly-T_{15} was similarly purchased with 6-FAM conjugated to the 5'-terminus.

Hybridization of the RNA-DNA scaffold

RNA-DNA hybridization was performed by mixing a 1:1 molar ratio of B1 RNA and splint DNA, each at 1μM, in hybridization buffer (10mM Tris pH 7.5, 200 mM NaCl, 1 mM EDTA), heating to 90°C for 1 min, cooling to 55°C for 3 min, and cooling to 4°C indefinitely.

Co-assembly of CCMV CP and the hybrid RNA-DNA scaffold – assembling the cherry bomb

Assembly was carried out as described in our earlier packaging studies involving CCMV CP and pure RNA[2–4]. Briefly, the RNA-DNA scaffold (final concentration 1nM) was mixed with purified CCMV CP in a ratio (wt/wt) of 6:1 in protein buffer and then dialyzed overnight at 4 °C against assembly buffer (50 mM NaCl, 10 mM KCl, 5 mM MgCl2, 1 mM DTT, 50 mM Tris-HCl pH 7.2). The samples were then dialyzed against virus suspension buffer (50 mM sodium acetate, 8 mM magnesium acetate pH 4.75) for at least 6 h to complete the assembly process. The products were then concentrated using a 100 kDa MWCO centrifugal filter device (EMD Milipore) operated at 3,000 g.

The yield of cherry bombs – the fraction of RNA-DNA hybrids that are packaged by protein into capsids, with the ssDNA end accessible outside – was difficult to quantify by direct visualization by TEM because of the faint signal from the exposed RNA-DNA fuse. The majority of the assembly products appeared as well-formed capsids, but the number of capsids with a clearly visible fuse (Fig. S1) was low. However, native agarose gel electrophoresis showed that equilibrating roughly equal molar concentrations of cherry bombs and fluorescently labeled poly-dT (Fig. 4) resulted in all of the poly-dT signal comigrating with the cherry bombs (see lane 3 of Fig. 4) – suggesting that most of the RNA-DNA hybrids were packaged and that the resulting cherry bombs had functional fuses.

Decorating 30-nm gold nanoparticles with short DNA strands

30-nm diameter gold nanoparticles (AuNPs) were functionalized following the protocol described by Hurst, Lytton-Jean, and Mirkin[5]. Briefly, 20 nmoles of 5' dithiol-terminated Poly-T_{25} DNA oligos (Integrated DNA Technologies) were incubated with DTT (0.1M DTT, 0.18M phosphate buffer, pH 8) for 1 hour at room temperature. The DTT was then removed with a Nap-5 column (Sephadex G-25 DNA Grade), and the purified oligo concentration was determined by UV-visible spectroscopy. 2 nmoles of deprotected, thiolated Poly-T_{25} oligos (final concentration of 1 μM) were added to 1 ml of 30 nm citrate-stabilized gold nanoparticles (Nanopartz Inc., OD=1, 0.05 mg/ml, final concentration of 300 pM) and the mixture was brought to 0.01M phosphate buffer pH 7, 0.01% SDS. The reaction was mixed and sonicated thoroughly, then incubated on a rotator for 2 hours in the dark. The conjugation mix was incrementally introduced to higher salt conditions in the following way: 12.5 μL of 2M NaCl was mixed thoroughly into the reaction vessel, followed by sonication and a 1 hour incubation. This procedure was repeated a total of 6 times, bringing the final concentration of NaCl to 0.1M. After salting, the reaction mix was left on a rotator overnight in the dark. To remove unbound DNA oligos, the solution was centrifuged at 10,000 g for 20 minutes, the supernatant was removed, and the gold nanoparticle pellet was resuspended in 1 ml 0.01M phosphate buffer pH 8, 0.1M NaCl, 0.01% SDS. This was repeated 3 times, and the final pellet resuspended in 0.01M phosphate buffer pH 8, 0.1M NaCl. The products were imaged by negative-stain TEM (Fig. S2), which revealed a faint ring of material surrounding the electron-dense AuNP that most likely corresponds to the DNA coat. The number of Poly-T_{25} oligos coating the nanoparticles was not quantified, but oligo-coating was tested qualitatively using a salt-stability assay.

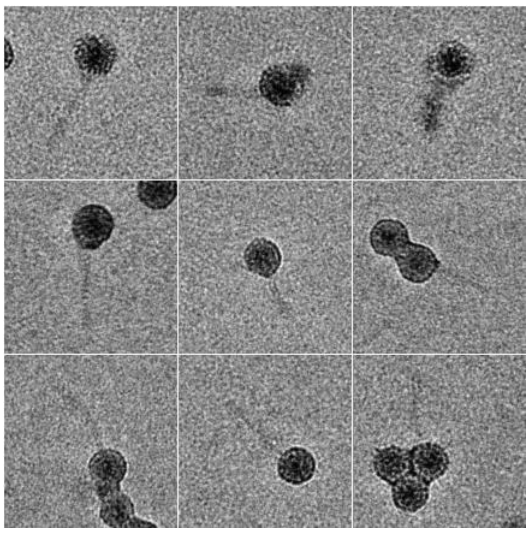

Figure S1. Positive stain TEM images of cherry bomb assembly products that show the ds-RNA-DNA "fuse".

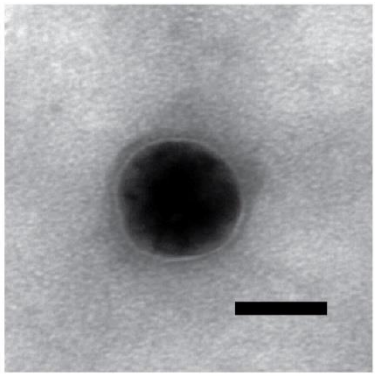

Figure S2. 30-nm AuNP coated with poly-T_{25} imaged by negative-stain TEM. Scale bar shows 25 nm.

Testing for non-specific binding between CCMV VLPs and poly-T_{25}-coated AuNPs

A control co-assembly reaction involving CCMV CP and pure B1 RNA was performed in parallel with the cherry bomb assembly reactions. The assembly products of the control reaction were then mixed with poly-T_{25}-coated AuNPs, equilibrated for 5 min on ice, and imaged by negative-stain TEM (Fig. S3). The same conditions were used to assess the binding of cherry bomb capsids with the poly-T_{25}-coated AuNPs. The control micrographs revealed no evidence of non-specific VLP-AuNP binding.

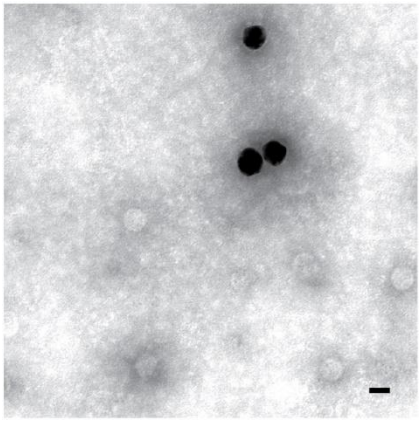

Figure S3. 30-nm AuNPs coated with poly-T_{25} (dark spheres) were incubated with VLPs containing pure B1 RNA (light spheres) and imaged by negative-stain TEM. There is no interaction between VLPs and AuNPs. Scale bar shows 25 nm.

Aggregated assembly of CP around surface-bound RNA

Hybridized RNA-DNA was prepared and equilibrated with 30-nm poly-T_{25}-coated AuNPs at a molar ratio of 10:1 (RNA:AuNP) for 30 min on ice. After hybridization of the RNA to the AuNPs, CP was added at a mass ratio of 10:1 (CP:RNA), equilibrated for 5 min on ice, and imaged by negative-stain EM (Fig. 5B). We used a higher amount of CP (compared to the 6-fold mass ratio used to completely package unbound RNA[3,4]) in case a fraction of the CP was bound by the excess of poly-T_{25} DNA oligos coating the surface of the AuNPs. Indeed, TEM images showing thickened layers of material coating the AuNP surface suggest that CP does bind the poly-T_{25}-coating (Fig. S4). Earlier assembly studies[3] using pure RNA showed that CP:RNA mass ratios higher than 6:1 can result in aggregation. This phenomenon may contribute to the aggregation we see in the AuNP-bound assemblies (Fig. S4).

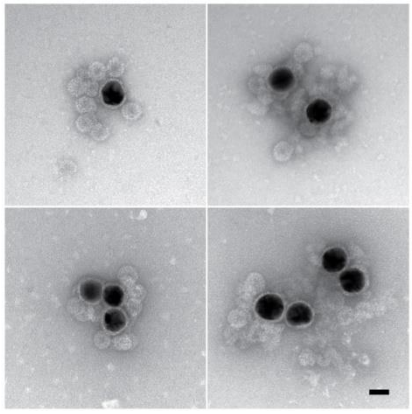

Figure S4. VLP assembly around RNA-DNA bound to the surface of 30-nm AuNPs coated with poly-T_{25} showed significant aggregation. The three types of aggregation seen are (i) an extra layer of material coating each AuNP (thick white halos surrounding electron-dense AuNP found in all images), (ii) extended capsid structures (upper-left image), and (iii) amorphous aggregation (upper-right and lower-right images). Scale bar shows 25 nm.

Transmission Electron microscopy (TEM)

Negative-stain: 6 µL of sample at a concentration of a few nM was deposited on glow-discharged copper grids (400-mesh) that previously had been coated with Parlodion and carbon. After 1 min, the grids were blotted and stained with 6 µL of 2% uranyl acetate for 1 min followed by blotting and storage in a desiccator overnight.

Positive stain: Inevitably, some regions of a negative-stained TEM grid exhibit positive staining. In these regions stain penetrates the sample particles, rather than coating them. We have found that certain structural features are sometimes better resolved through positive staining – in this case, the RNA-DNA hybrid appendage was more visible in positive-stained regions (Fig. S1).

Native agarose gel electophoresis

10 μL of sample was mixed with 3 μL of glycerol and loaded into a 1% agarose gel in virus electrophoresis buffer (0.1 M sodium acetate, 1 mM EDTA, pH 5.5). The samples were electrophoresed at 4°C at 50 V for 1 h and visualized with a FX Pro Plus Fluorimager/PhosphorImager (Bio-Rad) by exciting the UTP-AF488 of the B1 RNA and 6-FAM of the poly-T_{15}, separately, and measuring the emitted fluorescence intensity. The emission intensity of UTP-AF488 (RNA) is shown in red, and that of 6-FAM (poly-T) is shown in green.

REFERENCES

(1) Annamalai, P.; Rao, A. L. N. *Virology* **2005**, *332*, 650.
(2) Garmann, R. F.; Comas-Garcia, M.; Gopal, A.; Knobler, C. M.; Gelbart, W. M. *J. Mol. Biol.* **2014**, *426*, 1050.
(3) Cadena-Nava, R. D.; Comas-Garcia, M.; Garmann, R. F.; Rao, A. L. N.; Knobler, C. M.; Gelbart, W. M. *J. Virol.* **2012**, *86*, 3318.
(4) Garmann, R. F.; Comas-Garcia, M.; Koay, M. S.; Cornelissen, J. J.; Knobler, C. M.; Gelbart, W. M. *J. Virol.* **2014**, *88*, 10472.
(5) Hurst, S. J.; Lytton-Jean, A. K.; Mirkin, C. A. *Anal. Chem.* **2006**, *78*, 8313.